

GRASP and Path Relinking Hybridizations for the Point Matching-based Image Registration Problem

José Santamaría

Department of Computer Science, EPS de Linares, C/ Alfonso X El Sabio, 28, 23700 Linares, University of Jaén, Jaén, Spain, jslopez@ujaen.es

Oscar Cordon, Sergio Damas

European Centre for Soft Computing, Edif. Científico-Tecnológico C/ Gonzalo Gutiérrez Quirós, 33600 Mieres, Asturias, Spain, {oscar.cordon@softcomputing.es, sergio.damas@softcomputing.es}

Rafael Martí

Department of Statistics and Operations Research, Facultad de Matemáticas, C/ Dr. Moliner 50, 46100 Burjassot, Valencia, University of Valencia, Spain, rafael.marti@uv.es

R. Juan Palma

Department of Computer Science and Artificial Intelligence, ETSIIT, C/ Daniel Saucedo Aranda, 18071 Granada, University of Granada, Spain, odracirnumira@gmail.com

In the last decade, image registration has proven to be a very active research area when facing computer vision problems, specially in medical applications. In general, image registration methods aim to find a transformation between two images taken under different conditions. Point matching is an image registration approach based on searching for the right pairing of points between the two images, thus involving a combinatorial optimization problem. From this matching, the registration transformation can be inferred by means of numerical methods. In this paper, we tackle the medical image registration problem by means of a recent hybrid metaheuristic composed of two well-known optimization methods: GRASP and path relinking. Several designs based on this new combinatorial optimization approach have been tackled. Moreover, realistic and real-world cases of study of medical image registration problems have been considered. In particular, the experiments conducted in this work have shown the good performance of the combination between GRASP and evolutionary path relinking when compared to similar approaches of the state of the art of image registration.

Key words: metaheuristics; GRASP; path relinking; scatter search; computer vision; medical image registration;

History: Accepted by XXXX, former Area Editor for AAA; received June 2010; revised MM YYYY, MMM YYY; accepted MM YYYY.

1. Introduction

There are many applications in the digital image processing field (González and Woods, 2002) that require the proper alignment of different images (Goshtasby, 2005; Zitová and Flusser, 2003). These problems arise from rather different domains (Dasgupta and Banerjee, 2005; Kim et al., 2001; Wang, 2005). For example, in remote sensing, it is important to put into correspondence the images acquired from different viewpoints in order to achieve a global cartography from partial views. In medical imaging, it is helpful to determine a proper matching between the images provided by different kinds of sensors which are capable to highlight different characteristics of the human anatomy as bones, organs, or lesions.

In the last decade, image registration (IR) has become a fundamental task in computer vision commonly used to finding the correspondences (or transformations) among two or more images in order to achieve their proper alignment (Brown, 1992; Zitová and Flusser, 2003). There exist two different IR approaches (Cordón et al., 2007), each one working in a different solution space: i) to search for the optimal point matching between two images (Besl and McKay, 1992; Feldmar and Ayache, 1996; Cordón and Damas, 2006; Cordón et al., 2008; Liu, 2004); and ii) to directly search in the space of the registration transformation parameters (He and Narayana, 2002; Cordón et al., 2006a; Silva et al., 2005; De Falco et al., 2008; Yamany et al., 1999). While the former faces a combinatorial optimization approach, the latter does the same from a numerical (binary, integer, or real coded) optimization point of view (Cordón et al., 2007).

In particular, point matching searches for the right pairing of points between two images, from which the registration transformation can be inferred by using numerical methods (Horn, 1987). The main advantage of this IR approach is that it does not require the estimation of the suitable interval ranges of every parameter defining the transformation¹. Thus, the proposal of outstanding point matching algorithms is of importance in the IR community.

In this contribution, we extend our previous work (Cordón et al., 2008) and exploit the benefits of applying the recent hybridization (Resende et al., 2010) of the *greedy randomized adaptive search procedure* (GRASP) (Feo and Resende, 1995) and the *path relinking* (PR) algorithm (Resende and Werneck, 2004) when tackling point matching-based IR problems

¹In (Cordón et al., 2007), it is proven the poor performance obtained by some of the state of the art IR methods based on the transformation parameters approach when they consider a large search space.

of 3D medical images. Our contribution is two-fold. On the one hand, we aim to achieve a good trade-off between the intensification and diversification components of this hybrid approach in order to improve the problem solving. On the other hand, we aim to take advantage of heuristic information extracted from the images to guide the process with the same aim. Such information corresponds to the curvature values of the object under study and it has proven to be useful to achieve high quality solutions (Cordón and Damas, 2006; Cordón et al., 2007, 2008). Furthermore, curvature information facilitates a feature-based IR approach characterized by a significant reduction of input data which are represented by the most relevant points (according to this heuristic information) of the object, thus allowing a better matching and speeding up the IR process (Cordón et al., 2006b; Santamaría et al., 2009). It must be noted that the use of problem information is in line with previous findings in different metaheuristics (Glover, 1986; Glover and Kochenberger, 2003), such as tabu search (TS) (Glover and Laguna, 1997) and contrasts with random designs typically applied in other evolutionary methods.

The performance of several designs based on the hybridization of GRASP and PR algorithms is compared to our previous Scatter Search-based IR method (Cordón et al., 2008). To do so, we considered six 3D medical images from realistic and real-world image datasets with different modalities: magnetic resonance images (MRIs) of human brains and computer tomography images (CTs) of human wrists, respectively.

The structure of this paper is as follows. In Section 2 we describe the point matching-based IR problem viewed from a combinatorial optimization point of view. Section 3 is devoted to describe the recent hybridizations of GRASP and PR algorithms that we have adapted for tackling the IR problem. Computational experiments are detailed in Section 4. Finally, Section 5 presents concluding remarks and future works.

2. Point matching-based image registration

In this section the IR problem is formally described from a combinatorial optimization point of view. Besides, we detail the heuristic information and the permutation-based representation scheme exploited to guide the search process towards the best solutions for the point matching-based IR problem.

2.1. Problem formulation

IR can be stated as an NP-hard combinatorial optimization problem which consists of finding a mapping of points from two images: I_1 and I_2 , named scene and model, respectively. The objective is to determine the geometric transformation f that applied to I_1 leads it to I_2 (see Figure 1).

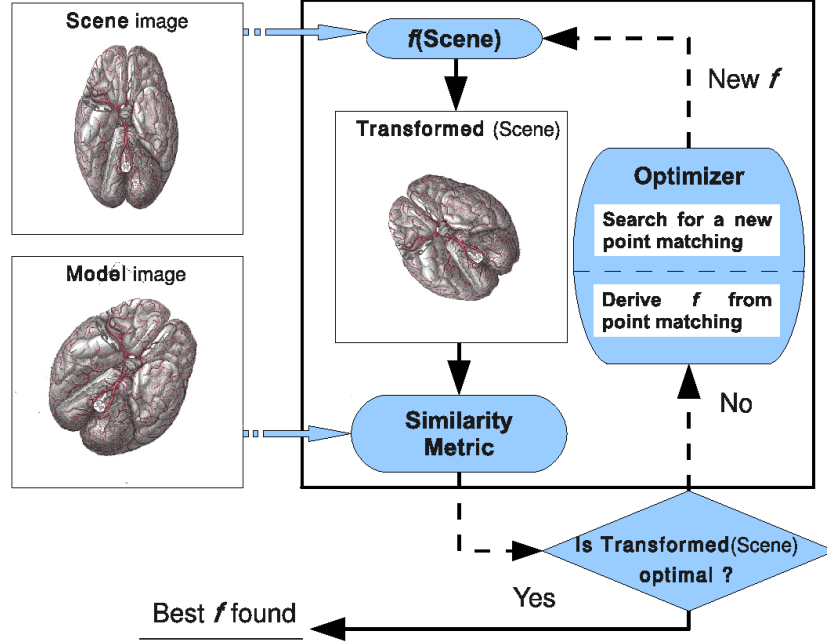


Figure 1: The IR optimization procedure

Typically, an image is represented by a huge amount of pixels/voxels (González and Woods, 2002). Therefore, many IR methods apply a preprocessing step to extract the most relevant geometric primitives (point, lines, etc) in the two images to be registered (Zitová and Flusser, 2003). This is called *feature-based* IR approach and takes the advantage of speeding up the IR process and better guiding the objective function to scape from local optima (Cordón et al., 2008). In particular, we consider points defining a crest line (Monga et al., 1992) as a set of geometric primitives extracted from both images I_1 and I_2 , noted P_1 and P_2 ($P_1 \subseteq I_1$, $P_2 \subseteq I_2$). Crest lines are the locus of points on a surface whose longest curvature (in absolute value) is locally maximal in the associated principal direction. Thus, a crest line can be viewed as a generalization of an edge for smooth surfaces in 3D (see Section 2.2).

In mathematical terms, point matching can be described as a combinatorial optimization problem as follows. Given two set of points $P_1 = \{\vec{x}_1, \vec{x}_2, \dots, \vec{x}_n\}$ and $P_2 = \{\vec{y}_1, \vec{y}_2, \dots, \vec{y}_m\}$, the

problem is to find a transformation f such that $\vec{y}_i = f(\vec{x}_{\pi(i)})$ for $i = 1, \dots, r$ ($r = \min(n, m)$), where $\pi = (\pi_1, \pi_2, \dots, \pi_l)$ is a permutation (see Section 2.3) of size l ($l = \max(n, m)$). Without loss of generality and to simplify the notation, we consider that P_1 is the largest point set, i.e., its dimension n is greater than that one of P_2 , m .

The problem solving is naturally divided into two phases. In the first one, a permutation of l elements defines the matching between the points in P_1 and P_2 in such a way that the first r elements ($r = m$ in our case) of π are the P_1 points associated to each of the m P_2 points. In the second phase, from the latter matching of points and using a numerical method (usually least squares estimation (Horn, 1987)), the parameters defining the transformation f are computed. The goal is to find the transformation minimizing the distances between the model points and the corresponding transformed scene points. Therefore, in optimization terms, the value associated with permutation π is given by the expression:

$$g(\pi) = \frac{\sum_{i=1}^r \|f_{\pi}(\vec{x}_{\pi(i)}) - \vec{y}_i\|^2}{r}, \quad (1)$$

i.e., $g(\pi)$ corresponds to the *Mean Square Error (MSE)*. Therefore, the point matching problem can be simply stated as minimizing $g(\pi)$ for any permutation π of l elements and its corresponding transformation f (Figure 2 illustrates the evaluation process).

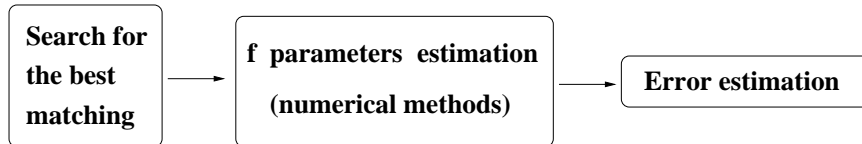


Figure 2: Point matching-based IR approach

2.2. Using heuristic information derived from the 3D image

This section is devoted to describe the heuristic information that can be derived from the curvature of the shapes included in the images in order to better address the optimization procedure of the IR problem.

Let us first define the iso-intensity surface of a 3D image, which will be called simply the iso-surface in the rest of this paper. For any continuous function $C(x, y, z)$ of \mathbb{R}^3 , any value I of \mathbb{R} (called the iso-value) defines a continuous, not self-intersecting surface, without hole, which is called the iso-intensity surface of C (Monga et al., 1992). A non ambiguous way to define the iso-surface is to consider it as being the surface which separates the space

regions where the intensity of C is greater or equal to I from these regions whose intensity is strictly lower than I . Whether such an iso-surface corresponds or not to the boundary of the scanned object is another problem, that will not be considered in the current contribution. Because of their good topological properties, iso-surface techniques are the most widely used methods of segmentation for 3D medical images.

Let us see now some properties of the iso-surfaces (see Figure 3). At each point \vec{x}_i of those surfaces, there is an infinite number of curvatures but, for each direction \vec{t} in the tangent plane at \vec{x}_i , there is only one associated curvature $k_{\vec{t}}$. There are two privileged directions of the surface, called the principal directions (\vec{t}_1 and \vec{t}_2), which correspond to the two extremal values of the curvature: k_1 and k_2 . We limit our model to these two parameters since they contain enough information to solve the IR problem.

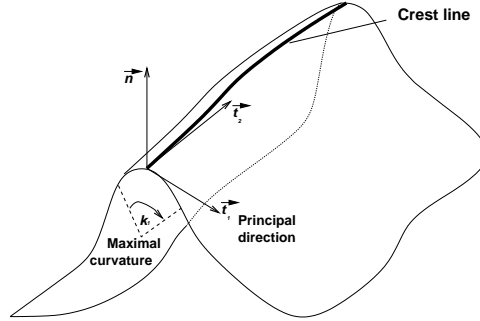


Figure 3: Differential characteristics of surfaces

As we will see next, this information is used in this work in a twofold way. On the one hand, the differences between the heuristic values of the matched points in the current solution are incorporated into the solution evaluation better to guide the search from a global perspective. On the other hand, they are taken into account in search strategies (e.g. the neighborhood operator of the local search mechanism) to intensify the search properly, as well as in the generation of high quality solutions with a large degree of diversity among them. In this way, we implement candidate list strategies in which permutations assigning feature points with similar heuristic values are ranked first, because they seem more promising than those with relatively different values. The consideration of this additional information in the point-matching process allows IR methods to obtain high quality solutions more quickly than other approaches.

2.3. Permutation-based point matching optimization

In our previous works (Cordón and Damas, 2006; Cordón et al., 2008), we developed point matching-based IR methods following a permutation-based combinatorial optimization approach. We implemented our solution method in such a way that the first r elements of the permutation ($r = m$ in our case) are the P_1 points associated to each of the m points in P_2 . Figure 4 illustrates these implementation details in which we can see that the P_1 points located between positions $r + 1$ and n are not assigned to any point in P_2 . Meanwhile, the first m points of the permutation define a matching between the small point set P_2 (of size m) and the large one P_1 (of size $n > m$); i.e., $\pi_{20} = 45$, defines a matching between the 20th point of P_2 (\vec{y}_{20}) and the 45th of P_1 ($\vec{x}_{\pi_{20}} = \vec{x}_{45}$), with $20 \leq m$ and $45 \leq n$.

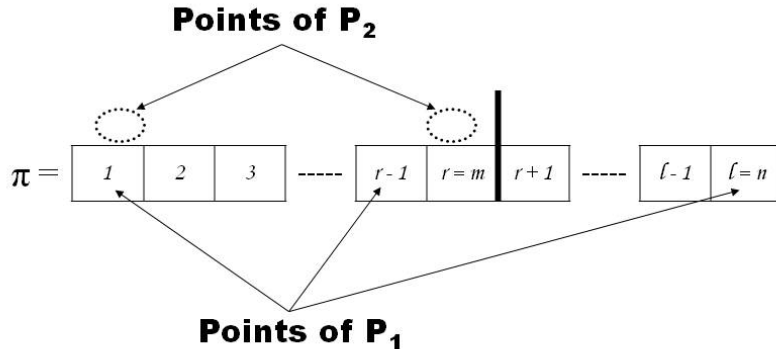


Figure 4: Implementation details of the point matching permutation π with size n

Then, we are able to infer the parameters of the registration transformation f relating the two 3D images, f_π , from the point matching π by means of computation of simple numerical methods such as the closed-form solution based on unit quaternion (Horn, 1987) solving a least-squares problem. In this contribution, we consider f to be a similarity transformation, thus being composed of a rotation $R = (\lambda, \langle \phi_x, \phi_y, \phi_z \rangle)$, a translation $\vec{t} = (t_x, t_y, t_z)$, and a uniform scaling s . Such a transformation has been extensively used to register aerial and satellite images, bony structures in medical images, and multimodal brain images (Gosh-tasby, 2005).

Next, once we know the expression of f_π , i.e., the (R, \vec{t}, s) parameters defining the similarity transformation, we can estimate the registration error existing between the scene image points \vec{x}_i and the model image points \vec{y}_j , measured by the $g()$ function as proposed in (Arun et al., 1987). We estimate the registration error by simply computing the

Euclidean distance from each transformed point in P_1 (using the aforementioned f_π parameters) to its corresponding matching point (considering π), as shown in Eq.(1), where $f_\pi(\vec{x}_{\pi_i}) = \vec{y} = s \cdot R(\vec{x}_{\pi_i}) + \vec{t}$.

Note that Eq.(1) computes only the geometric information of both scene and model feature points. Some authors ((Yamany et al., 1999; Luck et al., 2000; Robertson and Fisher, 2002)) have proposed several metaheuristic approaches that are aimed only at minimizing the $g()$ error function. However, by considering only this objective function, search algorithms suffer from several problems such as their inability to handle large initial misalignments between the two images, which usually makes the IR algorithm more likely to become trapped in local optima (Luck et al., 2000).

To overcome the latter pitfalls, problem-dependent (context) information can be used in the search method (Cordón and Damas, 2006; Cordón et al., 2008). To do so, we take into account the extracted curvature (heuristic) information (see Section 2.2). For each point \vec{x}_i , we consider the two values of the first and second principal curvatures, $k_1(\vec{x}_i)$ and $k_2(\vec{x}_i)$, associated with the two principal orthogonal directions (which locally characterize the iso-surface). An interesting quality of this feature is that curvature values represent an invariant source of information with respect to the similarity transformation f_π . Thus, a redefined function $m_{error}(\cdot)$ is additionally used in this paper in order to evaluate the quality of the matching stored in a given solution, π , as follows:

$$m_{error}(\pi) = \Delta k_1 + \Delta k_2 \quad \text{where} \quad \Delta k_j = \sum_{i=1}^r (k_j^i - k_j^{\pi_i})^2, \quad j = \{1, 2\}$$

where Δk_1 and Δk_2 measure the error associated to the matching of scene and model points with different values for the first and second principal curvatures, respectively.

Hence, the proposed objective function (similarity metric) for point matching makes use of a weighted combination of the $g()$ function (MSE of the registration transformation resulting from the point matching encoded in π) and the previous criterion based on heuristic information as follows:

$$\min F(\pi) = w_1 \cdot g(\pi) + w_2 \cdot m_{error}(\pi) \tag{2}$$

where w_1 and w_2 are weighting coefficients defining the relative importance of each term. With such a function, we defined a more suitable similarity measure to induce a better search process in the space of solutions (Cordón and Damas, 2006; Cordón et al., 2008).

3. Recent hybridizations of GRASP and path relinking and their adaptation to the point matching image registration problem

Our specific design of hybrids using GRASP and PR algorithms for the point matching-based IR problem² is based on the work carried out in (Resende et al., 2010), where the authors successfully tested several combinations of both metaheuristics facing the max-min diversity problem.

Several design aspects should be taken into account in order to achieve a suitable adaptation of these hybrid algorithms to the IR problem. In the next subsections, we first present some basis and the specific adaptation of both GRASP and PR metaheuristics to tackle the point matching-based IR problem. Then, several hybrid designs using both algorithms are described in detail.

3.1. The greedy randomized adaptive search procedure

The GRASP methodology was developed in the late 1980s (Feo and Resende, 1989, 1995). We refer the reader to (Resende and Ribeiro, 2003) for a recent survey of this metaheuristic. Each GRASP iteration consists of constructing a trial solution and then applying an improvement procedure to find a local optimum (i.e., the final solution for that iteration). The construction phase is iterative, greedy, and adaptive. It is iterative because the initial solution is built considering one element at a time. It is greedy because the addition of each element is guided by a greedy function. It is adaptive because the element chosen at any iteration in a construction is a function of those previously chosen. The improvement phase typically consists of a local search procedure.

Our adaptation of the GRASP methodology for the point matching problem is as follows. The information extracted from the shape of the object (see Section 2.2) can be used to establish a preference order for the assignments between the scene image points and the model image ones. Hence, a point \vec{x}_i from the scene image is more likely to be assigned to those model points \vec{y}_j presenting the same or similar curvature values k_1 and k_2 . In order to achieve that suitable point assignment, one possible approach consists of considering a greedy heuristic. Such approach is characterized by a strict selection order to assign the closest

²A very preliminar study facing the point matching problem by means of a particular hybridization of GRASP and PR algorithms has been previously presented at IEEE CEC 2010 (Santamaría et al., 2010).

model point \vec{y}_j in terms of curvature to every scene point \vec{x}_i , where \vec{y}_j was not previously assigned to some other scene point. However, we prefer to follow a different approach by introducing randomness in both processes thus allowing each decision to be taken randomly from the points still stored in the nonempty candidate list. Likewise, the latter procedure behaves similarly to a GRASP construction phase Resende and Ribeiro (2003).

As described in Section 2.3, a solution of our problem is characterized by a permutation π . The greedy randomized construction (GRC) phase of π starts by creating two candidate lists, CL_1 and CL_2 , related to the scene and model images, respectively. At the beginning, every list consists of all the points in the image (i.e., initially $CL_1 = P_1$ and $CL_2 = P_2$). For each element \vec{x}_i in CL_1 , its Euclidean distance to CL_2 in terms of curvature values is computed as:

$$d_i = \min_{j=1,\dots,m} \sqrt{(k_1(\vec{x}_i) - k_1(\vec{y}_j))^2 + (k_2(\vec{x}_i) - k_2(\vec{y}_j))^2} \quad (3)$$

Thus, d_i is the minimum value of the distances from \vec{x}_i to all the elements in CL_2 . Then, the GRC phase constructs the restricted candidate list RCL_1 with a percentage α of the elements in CL_1 with the lowest d_i (high quality) values. We randomly select one element (say \vec{x}_k) from RCL_1 for the matching assignment. In order to find an appropriate point in the model to match \vec{x}_k , we construct RCL_2 with a percentage α of the elements in CL_2 whose curvature values are closer to those of \vec{x}_k , i.e., those elements presenting the lowest distance values to \vec{x}_k . Next, we randomly select a point (say \vec{y}_t) in RCL_2 and match it to \vec{x}_k . The permutation π is accordingly updated with $\pi(t) = k$. Finally, we update CL_1 and CL_2 ($CL_1 = CL_1 - \{\vec{x}_k\}$, $CL_2 = CL_2 - \{\vec{y}_t\}$) and perform a new iteration. The GRC procedure finishes when $r = \min(n, m)$ points have been matched, i.e., when either CL_1 or CL_2 is empty, and the remaining $l - r$ points in the permutation π are taken randomly from the points still stored in the nonempty CL.

Different approaches for the GRC can be adopted (Resende et al., 2010). For instance, the GRC2 variant swaps the greedy and the randomization rules in the construction of the RCL (Resende and Werneck, 2004). This alternative design has been less studied in previous algorithms than the traditional greedy plus random method. Specifically, in our problem the restricted candidate list RCL_1 is built considering a percentage β of randomly chosen elements in CL_1 . Next, the element with the lowest d_i value is selected from RCL_1 . The same approach is followed for the construction of RCL_2 . Finally, another interesting variant is the parameter free version of GRC, called the reactive-GRC (RGRC), in which the value

of the parameter (α or β) is randomly determined according to an empirical distribution of probabilities (Prais and Ribeiro, 2000) identified in previous construction steps of the method.

Regarding to the local search (LS) phase of GRASP, we have used the strategy designed for the *Improvement Method* of the scatter search (SS)-based IR proposal designed in our previous work (Cordón et al., 2008). Therein the “best-first” LS procedure with the swapping neighbor operator is considered. In particular, swappings are used as the primary mechanism to move from one solution to another. Moreover, two improvements were considered in order to speed up the local search procedure. A primary strategy was applied first in the neighborhood generation by only considering promising swapping moves taking as a base the curvature (heuristic) information. Then, a selective application of the local optimizer was also considered.

3.2. Path relinking

PR (Glover, 1996; Glover and Laguna, 1997) was suggested as an approach to integrate intensification and diversification strategies in the context of TS. This approach generates new solutions by exploring trajectories that connect high quality solutions by starting from one of these solutions, called an *initiating solution*, and generating a path in the neighborhood space that leads toward the other solutions, called *guiding solutions*. This is accomplished by selecting moves that introduce attributes contained in the guiding solutions, and incorporating them in an *intermediate solution* initially originated in the initiating solution.

Later, PR was adapted in the context of GRASP as a form of intensification (Laguna and Martí, 1999). The relinking in this context consists of finding a path between a solution found with GRASP and a chosen elite solution. Therefore, the relinking concept has a different interpretation within GRASP since the solutions found from one GRASP iteration to the next are not linked by a sequence of moves (as in the case of TS). As can be seen in different sources (see for instance <http://twitter.com/graspheuristic>), the hybridization of GRASP with PR has revealed as a powerful metaheuristic that is able to provide high quality solutions for different combinatorial optimization problems.

Let π^1 and π^2 be two solutions of the point matching IR problem, interpreted as the sets of n selected elements Sel_{π^1} and Sel_{π^2} , respectively ($|Sel_{\pi^1}| = |Sel_{\pi^2}| = n$). $PR(\pi^1, \pi^2)$ starts with the first (initiating) solution π^1 , and gradually transforms it into the second (guiding) one π^2 by swapping out elements selected in π^1 with elements selected in π^2 . The elements

selected in both solutions π^1 and π^2 , $Sel_{\pi^1\pi^2}$, remain selected in the intermediate solutions generated in the path between them. Let $Sel_{\pi^1-\pi^2}$ be the set of elements selected in π^1 and not selected in π^2 . Symmetrically, let $Sel_{\pi^2-\pi^1}$ be the set of elements selected in π^2 and not selected in π^1 , i.e.

$$\begin{aligned} Sel_{\pi^1\pi^2} &= Sel_{\pi^1} \cap Sel_{\pi^2}, \\ Sel_{\pi^1-\pi^2} &= Sel_{\pi^1} \setminus Sel_{\pi^1\pi^2}, \\ Sel_{\pi^2-\pi^1} &= Sel_{\pi^2} \setminus Sel_{\pi^1\pi^2}. \end{aligned}$$

Let $\pi^{ini(0)} = \pi^1$ be the initiating solution. To obtain the solution $\pi^{ini(1)}$, we unselect a single element $\pi_i^{ini(0)} \in Sel_{\pi^1-\pi^2}$ and select a single element $\pi_j^{ini(1)} \in Sel_{\pi^2-\pi^1}$ both in $\pi^{ini(0)}$, thus obtaining:

$$Sel_{\pi^{ini(1)}} = Sel_{\pi^{ini(0)}} \setminus \{\pi_i^{ini(0)}\} \cup \{\pi_j^{ini(1)}\}.$$

In the *greedy PR* (PR^g) algorithm, the selection of the elements $\pi_i^{ini(0)}$ and $\pi_j^{ini(0)}$ is made in a greedy fashion. To obtain $\pi^{ini(k+1)}$ from $\pi^{ini(k)}$, we evaluate all the possibilities for $\pi_i^{ini(k)} \in Sel_{\pi^{ini(k)}-\pi^2}$ to be de-selected and $\pi_j^{ini(k)} \in Sel_{\pi^1-\pi^{ini(k)}}$ to be selected, and perform the best swap. In this way, we reach π^2 from π^1 in $h = |Sel_{\pi^1-\pi^2}| = |Sel_{\pi^2-\pi^1}|$ steps, i.e. $\pi^{ini(h)} = \pi^2$. The output of the PR algorithm is the best solution, different from π^1 and π^2 , found in the path connecting both solutions (among $\pi^{ini(1)}, \pi^{ini(2)}, \dots, \pi^{ini(h-1)}$).

Another variant of PR is based on a greedy randomized (PR^{gr}) scheme (Faria et al., 2005), in which the moves are done in a greedy randomized fashion. This procedure mimics the selection method employed in a GRASP construction. Instead of exploring all the possibilities for $\pi_i^{ini(k)} \in Sel_{\pi^{ini(k)}-\pi^2}$ to be de-selected and $\pi_j^{ini(k)} \in Sel_{\pi^1-\pi^{ini(k)}}$ to be selected to obtain $\pi^{ini(k+1)}$ from $\pi^{ini(k)}$, it can be performed a truncated exploration of a certain percentage of the whole neighborhood in order to speed up the run time. Thus, the candidate set C contains all these swaps, i.e.

$$C_{\pi^1\pi^2}^k = \{(\pi_i^{ini(k)}, \pi_j^{ini(k)}) \mid i \in Sel_{\pi^{ini(k)}-\pi^2}, \\ j \in Sel_{\pi^1-\pi^{ini(k)}}\}.$$

Let $z(i, j)$ be the value of the move associated with de-select $\pi_i^{ini(k)}$ and select $\pi_j^{ini(k)}$ in the current solution $\pi^{ini(k)}$ to obtain $\pi^{ini(k+1)}$. Then,

$$z(i, j) = F(\pi^{ini(k+1)}) - F(\pi^{ini(k)}).$$

In step k of the path from π^1 to π^2 , the restricted candidate list $RCL_{\pi^1\pi^2}^k$ of good candidates for swapping is

$$RCL_{\pi^1\pi^2}^k = \{(\pi_i^{ini(k)}, \pi_j^{ini(k)}) \in C_{\pi^1\pi^2}^k \mid z(i, j) \geq \delta z^*\},$$

where z^* is the minimum of $z(i, j)$ in $C_{\pi^1\pi^2}^k$ and δ ($0 \leq \delta \leq 1$) is a search parameter. A pair $(\pi_i^{ini(k)}, \pi_j^{ini(k)}) \in RCL_{\pi^1\pi^2}^k$ is randomly selected and the associated swap is performed.

On the other hand, PR can be performed in a bidirectional manner by exploring the two possible paths connecting two given solutions. The best solution found is accordingly returned. Moreover, an improved performance regarding the computation time can be achieved by considering a pruning scheme for the neighborhood exploration of PR by using the heuristic information extracted from the image. We refer the reader to (Cordón et al., 2008) for a more detailed description of the latter intelligent strategy.

3.3. Static hybridization of GRASP and PR

In Stc-G&PR, we propose a static hybridization in which we first apply GRASP to construct the elite set (ES) (see steps 1 to 14 in Figure 5) and then, as a second step, we apply PR to generate solutions between all the pairs of solutions in ES (see steps 15 to 24 in Figure 5). As shown in Figure 5, we always keep the best solution in ES (π^1) during the realization of the GRASP and the LS phases. We should remark the use of a distance that is considered to measure how diverse one solution is with respect to a set of solutions, ES in this case. Specifically, for the point matching we consider the distance between two permutations π^a and π^b as the number of times $\pi_{(i)}^a$ differs from $\pi_{(i)}^b$ for $i = 1, \dots, r$ (Cordón et al., 2008). Then, in Stc-G&PR and subsequents, the candidate solution π' is considered for inclusion in ES following a similar criteria as used in (Resende et al., 2010). In this case, either it has a better quality (according to $F()$ value) than the current best in ES (π^1), or it has a better quality than the current worst in ES (π^b) and it also increases the diversity of ES ($Div(ES)$) by means of replacing $\pi^k \in ES$ with π' ($ES \leftarrow \{ES \setminus \pi^k\} \cup \pi'$). In the second step of the algorithm, for each pair of solutions $\{\pi^a, \pi^b\} \in ES$, we apply PR in a bidirectional manner, i.e. $PR(\pi^a, \pi^b)$ and $PR(\pi^b, \pi^a)$. Next, the best solution generated in both paths is subjected to the LS method used in GRASP (see Section 3.1). Stc-G&PR stops once PR is applied to all the pairs in ES and the best overall solution x^{best} is returned as the output.

Unlike in (Resende et al., 2010), in our specific implementation of point matching the d th parameter (which is a distance threshold value that reflects the term “sufficiently different”

```

Begin Stc-G&PR
1  GlobalIter ← number of global iterations;
2  Apply GRASP (construction and local search) for  $b = |ES|$  iterations to populate
    $ES \leftarrow \{\pi^1, \pi^2, \dots, \pi^b\}$ ;
3  NumIter ←  $b+1$ ;
4  While NumIter ≤ GlobalIter Do
5      $\pi \leftarrow$  GRASP construction phase;
6      $\pi' \leftarrow$  GRASP LS starting at  $\pi$ ;
7      $\pi^k \leftarrow$  closest solution to  $\pi'$  in  $ES$  with  $F(\pi') < F(\pi^k)$ ;
8      $ES' \leftarrow \{ES \setminus \pi^k\} \cup \pi'$ ;
9     If  $F(\pi') < F(\pi^1)$  Or ( $F(\pi') < F(\pi^b)$  And  $Div(ES') \geq Div(ES)$ ) Then
10        Add  $\pi'$  to  $ES$  and remove  $\pi^k$ ;
11        Sort  $ES$  from best  $\pi^1$  to worst  $\pi^b$ ;
12    End-If;
13    NumIter ← NumIter + 1;
14 End-While;
15  $\pi^{best} \leftarrow \pi^1$ ;
16 For  $i = 1, \dots, b - 1$  Do
17    For  $j = i + 1, \dots, b$  Do
18        Apply  $PR(\pi^i, \pi^j)$  and  $PR(\pi^j, \pi^i)$  and let  $\pi'$  be the best solution found;
19         $\pi'' \leftarrow$  GRASP LS starting at  $\pi'$ ;
20        If ( $F(\pi'') < F(\pi^{best})$ ) Then
21             $\pi^{best} \leftarrow \pi''$ ;
22        End-If;
23    End-For;
24 End-For;
25 Return  $\pi^{best}$ ;

End-Stc-G&PR

```

Figure 5: Pseudo-code of the Stc-G&PR algorithm

and it should be empirically adjusted) has been properly removed from Stc-G&PR (see line 9 in Figure 5) as well as from the subsequent hybrids.

3.4. Dynamic hybridization of GRASP and PR

Another alternative of hybrid implementation using GRASP and PR algorithms consists of a dynamic update of ES, we called here Dyn-G&PR. In this design, each solution π' generated with GRASP is directly subjected to the PR algorithm, which is applied between π' and a solution π^j randomly selected from ES. As done in Stc-G&PR, the LS method is applied to the output of PR. In this case, the resulting solution is directly tested for inclusion in ES. If successful, it can be used as a guiding solution in later applications of PR. Figure 6 shows pseudo-code for this dynamic variant.

<pre> Begin Dyn-G&PR 1 <i>GlobalIter</i> \leftarrow number of global iterations; 2 Apply GRASP (construction and local search) for $b = ES$ iterations to populate $ES \leftarrow \{\pi^1, \pi^2, \dots, \pi^b\}$; 3 <i>NumIter</i> \leftarrow b+1; 4 While <i>NumIter</i> \leq <i>GlobalIter</i> Do 5 $\pi \leftarrow$ GRASP construction phase; 6 $\pi' \leftarrow$ GRASP LS starting at π; 7 Randomly select π^j from <i>ES</i>; 8 Apply PR(π', π^j) and PR(π^j, π') and let π'' be the best solution found; 9 $\pi''' \leftarrow$ GRASP LS starting at π''; 10 $\pi^k \leftarrow$ closest solution to π''' in <i>ES</i> with $F(\pi''') < F(\pi^k)$; 11 $ES' \leftarrow \{ES \setminus \pi^k\} \cup \pi'''$; 12 If $F(\pi''') < F(\pi^1)$ Or ($F(\pi''') < F(\pi^b)$ And $Div(ES') \geq Div(ES)$) Then 13 Add π''' to <i>ES</i> and remove π^k; 14 Sort <i>ES</i> from best π^1 to worst π^b; 15 End-If; 16 <i>NumIter</i> \leftarrow <i>NumIter</i> + 1; 17 End-While; 18 $\pi^{best} \leftarrow \pi^1$; 19 Return π^{best}; End-Dyn-G&PR </pre>
--

Figure 6: Pseudo-code of the Dyn-G&PR algorithm

3.5. Evolutionary GRASP and PR

In Evo-G&PR, the synergy between GRASP and evolutionary PR (EvoPR) proven to be a promising approach for combinatorial optimization problems (Resende and Werneck, 2004).

EvoPR was introduced in Evo-G&PR as a post-processing phase for GRASP with PR (Andrade and Resende, 2007). As in Dyn-G&PR, in each iteration of the algorithm (see Figure 7), the construction and the improvement phase of GRASP as well as the PR method are applied (see steps 5 to 9 in Figure 7) to obtain ES. After a number of iterations previously established, the GRASP with PR^g stops. In the post-processing phase (evoPR), PR is applied to each pair of solutions in ES (in steps 17 to 30). The solutions obtained with the latter application of PR are considered candidates to enter ES (following the updating criteria used in SS for the Reference Set (Cordón et al., 2008)), and PR is again applied to them as long as new solution is able to enter ES. Hence, solutions in ES evolve and the method stops when no new solutions update ES.

4. Experiments

This section is devoted to perform an experimental study of the previously described hybrid optimization approaches to tackle medical IR problems. The structure of this section is as follows: first, we introduce the medical image datasets in Section 4.1; next, preliminary experiments are conducted in Sections 4.2 and 4.3 in order to achieve the best tuning of the GRASP and PR algorithms; Sections 4.4 and 4.5 are devoted to perform an empirical study of the effectiveness and the robustness of the designed IR methods. In those sections, their performance is also compared to the IR methods of the state-of-the-art, in particular to our previous contribution based on SS (Cordón et al., 2008). We consider the MSE (Eq. 1) value for evaluation of IR results.

All the IR methods have been developed using C/C++ programming and tested in the same architecture using a 2.26GHz Intel® Core™2 Duo P8400 and a MS® Windows operating system.

4.1. Medical image datasets

Our results correspond to a number of registration problems for six medical images from two different image datasets. The first dataset is composed of four different magnetic resonance images (MRIs). These images have been obtained from the *BrainWeb* database at McGill University (Kwan et al., 1999). The purpose of this repository is to provide researchers with ground truth data for image analysis techniques and algorithms. *BrainWeb* has been widely used by the IR research community (see, for example, (Wachowiak et al., 2004)). One of

```

Begin Evo-G&PR
1  GlobalIter  $\leftarrow$  number of global iterations;
2  Apply GRASP (construction and local search) for  $b = |ES|$  iterations to populate
    $ES \leftarrow \{\pi^1, \pi^2, \dots, \pi^b\}$ ;
3  For  $iter = 1, \dots, GlobalIter$  Do
4      For  $i = 1, \dots, LocalIter$  Do
5           $\pi \leftarrow$  GRASP construction phase;
6           $\pi' \leftarrow$  GRASP LS starting at  $\pi$ ;
7          Randomly select  $\pi^j$  from  $ES$ ;
8          Apply  $PR(\pi', \pi^j)$  and  $PR(\pi^j, \pi')$  and let  $\pi''$  be the best solution found;
9           $\pi''' \leftarrow$  GRASP LS starting at  $\pi''$ ;
10          $\pi^k \leftarrow$  closest solution to  $\pi'''$  in  $ES$  with  $F(\pi''') < F(\pi^k)$ ;
11          $ES' \leftarrow \{ES \setminus \pi^k\} \cup \pi'''$ ;
12         If  $F(\pi''') < F(\pi^1)$  Or ( $F(\pi''') < F(\pi^b)$  And  $Div(ES') \geq Div(ES)$ ) Then
13             Add  $\pi'''$  to  $ES$  and remove  $\pi^k$ ;
14             Sort  $ES$  from best  $\pi^1$  to worst  $\pi^b$ ;
15         End-If;
16     End-For;
17      $NewSol \leftarrow 1$ ;
18     While  $NewSol$  Do
19          $NewSol \leftarrow 0$ ;
20         Apply  $PR(\pi, \pi')$  and  $PR(\pi', \pi)$  for every pair  $(\pi, \pi')$  in  $ES$  not combined
           before. Let  $\pi''$  be the best solution found;
21          $\pi''' \leftarrow$  GRASP LS starting at  $\pi''$ ;
22          $\pi^k \leftarrow$  closest solution to  $\pi'''$  in  $ES$  with  $F(\pi''') < F(\pi^k)$ ;
23          $ES' \leftarrow \{ES \setminus \pi^k\} \cup \pi'''$ ;
24         If  $F(\pi''') < F(\pi^1)$  Or ( $F(\pi''') < F(\pi^b)$  And  $Div(ES') \geq Div(ES)$ ) Then
25             Add  $\pi'''$  to  $ES$  and remove  $\pi^k$ ;
26             Sort  $ES$  from best  $\pi^1$  to worst  $\pi^b$ ;
27              $NewSol \leftarrow 1$ ;
28              $\pi^{best} \leftarrow \pi^1$ ;
29         End-If;
30     End-While;
31 End-For;
32 Return  $\pi^{best}$ ;

End-Evo-G&PR

```

Figure 7: Pseudo-code of the Evo-G&PR algorithm

the most important challenges associated to the current experimentation is that the goal of the IR process is to register *pairs of different images from the same object*. Therefore, we tackle a more realistic problem in medical IR, named *intra-subject registration*, than the one considered in (Cordón and Damas, 2006). The other two images considered belong to a second dataset of a real-world medical case of study kindly provided by the Rhode Island Hospital (Marai et al., 2006). Both are computerized tomography (CT) images of two different human wrists. In this case, we want to highlight the complexity of the problem to be tackled due to its particular anatomical structure.

As said, we followed a feature-based IR approach. After preprocessing the six images (I_1 to I_6), 583, 393, 348, 284, 575, and 412 crest line points are obtained, respectively.

The first column of Figures 8 and 9 show the original MRIs and CTs, respectively. The second column of those figures corresponds to the isosurfaces segmenting the original images to extract the regions of interest of each image, i.e. the brain and the wrist. The third column shows the crest line points extracted from each 3D medical image.

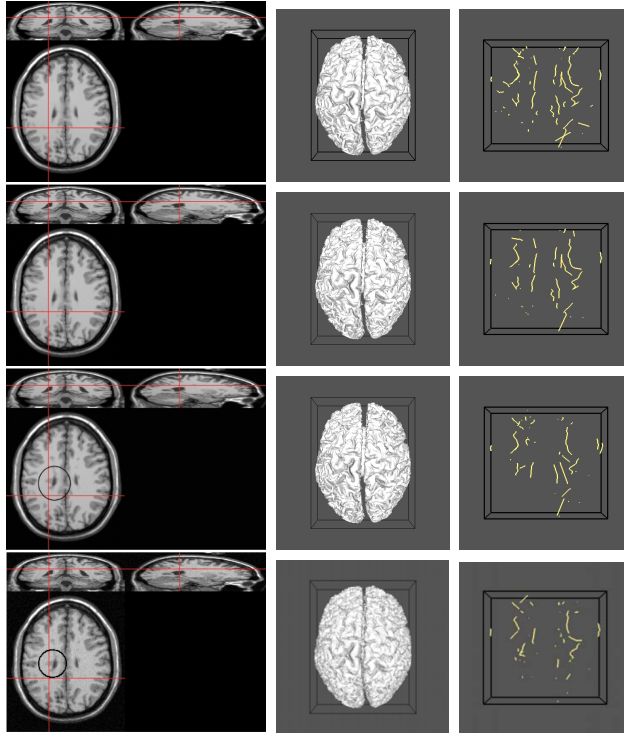


Figure 8: From left to right, and top to bottom: original MRI images, their respective isosurfaces, and their crest lines points. Note that the second and third MRIs include 1% of Gaussian noise while the fourth one has a 5%. I_3 and I_4 (last two rows) also considers a multiple sclerosis lesion (see circle)

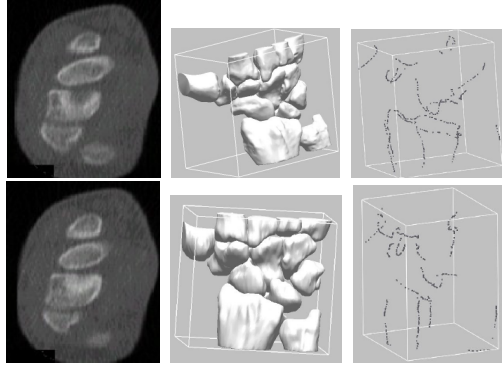


Figure 9: From left to right: original CT images, their respective isosurfaces, and their crest lines points. The first and second rows refer to I_5 and I_6 , respectively

In order to evaluate the performance of the IR methods tested, we considered four similarity transformations (see Section 2.3) T_i (see Table 1), each one describing a different level of misalignment between a pair of images (Cordón and Damas, 2006).

Table 1: Similarity transformations considered

	T_1	T_2	T_3	T_4
λ	115.0	168.0	235.0	276.9
ϕ_x	-0.863868	0.676716	-0.303046	0.872872
ϕ_y	0.259161	-0.290021	-0.808122	0.436436
ϕ_z	0.431934	0.676716	0.505076	-0.218218
t_x	-26.0	6.0	16.0	12.0
t_y	15.5	5.5	-5.5	5.5
t_z	-4.6	-4.6	-4.6	-24.6
s	1.0	0.8	1.0	1.2

4.2. Fine tuning of GRASP

The first preliminar experiment is devoted to select the best setup for the GRASP approach before it could be considered for inclusion in the previously described hybrids (see Sections 3.3 to 3.5). Sections 4.2.1 and 4.2.2 are devoted to perform the experimental design and the subsequent analysis of results, respectively.

4.2.1. Experimental design

We compared the performance of GRC and GRC2 for $\alpha, \beta \in \{0.75, 0.9, 0.95\}$, and their reactive versions, i.e. reactive-GRC (RGRC) and reactive-GRC2 (RGRC2). To do so, sixteen

IR problem instances (see Table 2) have been designed from the combination of the considered image datasets of MRIs of human brains and the four similarity transformations (see Figure 8 and Table 1, respectively). Each of the latter four variants of GRASP has been run once considering a maximum of one hundred iterations of the construction and the LS phases. We keep the same parameter settings for the LS method as done in (Cordón et al., 2008).

Table 2: The sixteen IR problem instances designed considering the realistic case of study of human brains, with $T_i = T_1, \dots, T_4$ (see Table 1)

IR problem	Scene image		Model image	
	Lesion	Noise	Lesion	Noise
I_1 vs $T_i(I_2)$	No	No	No	1%
I_1 vs $T_i(I_3)$	No	No	Yes	1%
I_1 vs $T_i(I_4)$	No	No	Yes	5%
I_2 vs $T_i(I_4)$	No	1%	Yes	5%

4.2.2. Analysis of results

Both the first (*#better*) and the second (*Divergence*) rows in Table 3 shows the averaged value of: i) the percentage of times in which a given GRC variant achieved a solution as better³ as the best found so far in each of the one hundred iterations; and ii) the divergence of a given GRC variant to the best GRC variant according to MSE values. From the obtained results, we remark that the GRC variant considering $\alpha = 0.9$ is the best alternative for the construction of solutions for GRASP. Thus, this will be our choice for the subsequent experiments.

Table 3: Results obtained by each of the eight considered variants of GRC.

	$GRC_{0.75}$	$GRC_{0.9}$	$GRC_{0.95}$	$RGRC$	$GRC_{20.75}$	$GRC_{20.9}$	$GRC_{20.95}$	$RGRC2$
<i>#better</i> (%)	3	11	8	8	2	0	0	9
<i>Divergence</i>	7.63	1.81	4.93	6.48	33.88	50.05	67.87	4.90

³We considered that a given solution is as better as the best found when its MSE value is only a 5% worse than the latter.

4.3. Fine tuning of Path relinking

As done in the previous section, this second preliminary experiment is devoted to study the best configuration of PR when it is hybridized with GRASP. To do so, Sections 4.3.1 and 4.3.2 are devoted to perform the experimental design and the subsequent analysis of results, respectively.

4.3.1. Experimental design

Here, we considered the Stc-G&PR approach (see Section 3.3). We included the best configuration of GRASP obtained in Section 4.2 and compared different variants of Stc-G&PR using the following designs of PR (see Section 3.2):

- PR_1 : PR^g & unidirectional⁴
- PR_2 : PR^g & bidirectional
- PR_3 : PR_1 & pruning the 30% of the path
- PR_4 : PR_1 & pruning the 50% of the path
- PR_5 : PR_2 & pruning the 30% of the path
- PR_6 : PR_2 & pruning the 50% of the path
- PR_7 : PR^{gr} & unidirectional
- PR_8 : PR^{gr} & bidirectional
- PR_9 : PR_7 & pruning the 30% of the path
- PR_{10} : PR_7 & pruning the 50% of the path
- PR_{11} : PR_8 & pruning the 30% of the path
- PR_{12} : PR_8 & pruning the 50% of the path

⁴An unidirectional scheme considers the construction of one solution following the route that connects the initial with the guiding solution. On the other hand, a bidirectional scheme performs the construction of two solutions considering the two possible routes (i.e. from the initial to the guiding solution, and the reverse route) and the best one is accordingly selected.

We also tested the latter twelve versions of PR considering a pruning scheme which makes use of the heuristic information for the exploration of the neighborhood (see Section 3.2). To develop this experimental study, four different IR problem instances (see Table 4) have been designed from the combination of the MRIs of human brains and the four similarity transformations (see Figure 8 and Table 1, respectively). The size of the ES set was set to 6 ($b = |ES| = 6$ solutions). Each of the latter twelve variants of Stc-G&PR has been run once considering, in this case, a maximum CPU time of 600 seconds.

Table 4: The four IR problem instances designed considering the realistic case of study of human brains, with $T_i = T_1, \dots, T_4$ (see Table 1)

IR problem	Scene image		Model image	
	Lesion	Noise	Lesion	Noise
I_1 vs $T_1(I_2)$	No	No	No	1%
I_1 vs $T_2(I_3)$	No	No	Yes	1%
I_1 vs $T_3(I_4)$	No	No	Yes	5%
I_2 vs $T_4(I_4)$	No	1%	Yes	5%

4.3.2. Analysis of results

Table 5 depicts the statistical results achieved by each of the variants of PR when tackling every of the four IR problem instances (e.g., I_1 vs. $T_1(I_2)$, I_1 vs. $T_2(I_2)$, I_1 vs. $T_3(I_2)$, and I_1 vs. $T_4(I_2)$) of their corresponding scenario (I_1 vs. $T_i(I_2)$). According to mean values, despite PR_{10} (which makes use of a greedy randomized scheme for movement selection of PR and follows a pruning scheme of the 50% of the unidirectional path), we can see how the remaining of the PR variants offer a better performance when the pruning scheme is not considered. The latter behavior is corroborated by the higher values of the standard deviation obtained when such a scheme is used. Regarding the minimum and the mean MSE values, it is proven that PR_{10} is the best choice among all the variants. Thus, we will consider this variant for the subsequent experiments.

4.4. Comparison with previous methods

The third experiment aims to analyze the effectiveness of each of the three hybrids based on GRASP and PR. Sections 4.4.1 and 4.4.2 are devoted to perform the experimental design and the subsequent analysis of results, respectively.

Table 5: MSE results obtained by each of the twelve variants of PR when using or not a pruning scheme

	without pruning				with pruning			
	<i>min</i>	<i>max</i>	μ	σ	<i>min</i>	<i>max</i>	μ	σ
PR_1	51.00	140.55	84.43	34.04	53.18	170.58	95.03	46.04
PR_2	52.13	129.89	82.32	32.59	47.51	149.08	87.69	40.35
PR_3	51.44	172.71	89.79	49.37	47.44	188.07	96.58	54.82
PR_4	48.10	140.84	92.08	43.24	45.72	249.35	117.29	81.99
PR_5	46.04	133.51	80.46	36.14	<u>43.11</u>	153.79	96.18	45.58
PR_6	53.82	164.15	89.88	44.52	55.58	151.83	85.21	39.30
PR_7	52.74	160.49	89.82	43.18	43.74	150.94	87.68	42.87
PR_8	52.93	154.38	89.42	38.80	52.71	127.10	<u>82.39</u>	27.35
PR_9	<u>44.31</u>	168.62	89.27	49.29	54.60	139.12	91.08	35.86
PR_{10}	45.49	141.22	<u>78.14</u>	38.56	45.08	148.52	93.92	43.40
PR_{11}	47.34	153.65	86.05	43.02	57.52	170.12	96.81	45.36
PR_{12}	47.29	136.64	82.12	35.54	45.55	150.30	83.15	41.19

4.4.1. Experimental design

Specifically, we included the best setup for GRASP and PR (see Sections 4.2 and 4.3, respectively) for Stc-G&PR, Dyn-G&PR, and Evo-G&PR in order to provide a fair comparison between the hybrids. Moreover, we also included a pure GRASP (using GRC and $\alpha = 0.9$) and our previous contribution based on SS as point matching-based IR method of the state-of-the-art (Cordón et al., 2008) as baselines for the latter methods' performance. To do so, we used the previously considered (see Section 4.2) IR problem instances (see Table 2). Each of the five IR methods has been run once considering a maximum CPU time of 600 seconds. We maintained the same parameter settings for the SS-based IR method used in (Cordón et al., 2008).

4.4.2. Analysis of results

Table 6 is split into four subtables considering every IR problem scenario (I_1 vs. $T_i(I_2)$, I_1 vs. $T_i(I_3)$, I_1 vs. $T_i(I_4)$, and I_2 vs. $T_i(I_4)$). The best MSE value is shown in underlined bold font for each of the sixteen IR problem instances. We remark the poor performance obtained by the pure GRASP which only achieves the best MSE value in one of the sixteen instances. On the contrary, the hybrid GRASP with PR variants proposed for point matching-based IR achieved competitive results when compared to the state-of-the-art algorithm based on

SS, which obtained the best MSE value in six of the sixteen instances. The remaining best MSE values (nine) were shared out amongst the three proposed hybrids. Specifically, Table 7 shows how both the SS and the Evo-G&PR methods achieve the best averaged effectiveness when facing the point matching IR problem. Hence, we can see how Evo-G&PR obtains high quality solutions for the IR problem as it has previously done in other challenging problems (Resende and Werneck, 2004; Resende et al., 2010).

Table 6: MSE values obtained by the three hybrids (Stc-G&PR, Dyn-G&PR, and Evo-G&PR), the pure GRASP, and the state-of-the-art IR algorithm based on SS for the IR problem instances in Table 4

T_1	Stc-G&PR	Dyn-G&PR	Evo-G&PR	GRASP	SS	T_2	Stc-G&PR	Dyn-G&PR	Evo-G&PR	GRASP	SS
	39.06	45.39	43.86	46.22	40.45		27.64	42.63	42.66	31.32	40.43
I_1 vs. $T_i(I_2)$											
T_3	Stc-G&PR	Dyn-G&PR	Evo-G&PR	GRASP	SS	T_4	Stc-G&PR	Dyn-G&PR	Evo-G&PR	GRASP	SS
	57.14	73.16	73.48	48.43	73.07		47.53	51.03	50.49	67.62	48.18
I_1 vs. $T_i(I_3)$											
T_1	Stc-G&PR	Dyn-G&PR	Evo-G&PR	GRASP	SS	T_2	Stc-G&PR	Dyn-G&PR	Evo-G&PR	GRASP	SS
	77.34	77.30	79.44	115.76	86.33		53.34	44.25	46.30	55.49	44.83
T_3	Stc-G&PR	Dyn-G&PR	Evo-G&PR	GRASP	SS	T_4	Stc-G&PR	Dyn-G&PR	Evo-G&PR	GRASP	SS
	93.11	76.87	64.70	116.26	66.42		125.32	107.90	109.92	170.59	112.36
I_1 vs. $T_i(I_4)$											
T_1	Stc-G&PR	Dyn-G&PR	Evo-G&PR	GRASP	SS	T_2	Stc-G&PR	Dyn-G&PR	Evo-G&PR	GRASP	SS
	65.26	88.63	91.47	118.74	79.59		60.85	36.35	39.18	84.03	36.32
T_3	Stc-G&PR	Dyn-G&PR	Evo-G&PR	GRASP	SS	T_4	Stc-G&PR	Dyn-G&PR	Evo-G&PR	GRASP	SS
	85.96	63.98	62.11	111.09	64.90		104.41	83.80	82.19	139.46	81.02
I_2 vs. $T_i(I_4)$											
T_1	Stc-G&PR	Dyn-G&PR	Evo-G&PR	GRASP	SS	T_2	Stc-G&PR	Dyn-G&PR	Evo-G&PR	GRASP	SS
	107.44	88.59	87.91	113.93	83.41		54.07	44.58	41.44	72.33	38.83
T_3	Stc-G&PR	Dyn-G&PR	Evo-G&PR	GRASP	SS	T_4	Stc-G&PR	Dyn-G&PR	Evo-G&PR	GRASP	SS
	105.50	88.40	87.82	131.17	86.48		117.86	92.13	92.69	179.37	78.70

Table 7: Overall effectiveness of each of the IR methods averaging their corresponding sixteen MSE values from Table 6

	Stc-G&PR	Dyn-G&PR	Evo-G&PR	GRASP	SS
μ	76.37	69.06	68.48	100.11	66.33

4.5. Evaluation of the robustness of proposed hybrid designs

Similarly as done in the previous section, this last experiment analyzes the robustness of the three designed and tuned hybrids. To do so, Sections 4.5.1 and 4.5.2 are devoted to perform the experimental design and the subsequent analysis of results, respectively.

4.5.1. Experimental design

We again considered our three GRASP and PR hybridization-based IR proposals as well as the pure GRASP and our previous contribution based on SS (Cordón et al., 2008). In this case, we enriched the IR problem instances by including the real-world case of study based on the image dataset of human wrists of CTs. Specifically, we considered the five IR problem instances shown in Table 8. Each of the five IR methods has been run⁵ ten times considering a maximum CPU time of 600 seconds.

Table 8: The five IR problem instances designed considering realistic and real-world cases of study of human brains and human wrists, respectively

IR problem	Scene image		Model image	
	Lesion	Noise	Lesion	Noise
I_1 vs $T_1(I_2)$	No	No	No	1%
I_1 vs $T_2(I_3)$	No	No	Yes	1%
I_1 vs $T_3(I_4)$	No	No	Yes	5%
I_2 vs $T_4(I_4)$	No	1%	Yes	5%
I_6 vs $T_1(I_5)$	–	–	–	–

⁵Each run uses a different seed for the pseudo-random number generator in order to avoid the bias of randomness.

4.5.2. Analysis of results

From Table 9, we can notice how the Evo-G&PR-based IR method achieves a competitive performance compared to the state-of-the-art IR algorithm based on SS. Specifically, the former algorithm achieves the best mean results for three of the five IR problem instances. Moreover, it obtains the lowest standard deviation values in all the cases. Therefore, Evo-G&PR-based provides a good trade-off between search space diversification and intensification, thus showing a more robust behavior than the SS-based IR method, the pure GRASP, and its counterpart hybrids: Stc-G&PR and Dyn-G&PR. Regarding to the accuracy of the approaches (i.e. minimum value of MSE), both SS and Evo-G&PR IR methods behave in a very similar way obtaining accurate results when tackling IR problem instances involving MRIs. The last row in Table 9 shows the averaged/overall performance (regarding the mean value of MSE) of each of the compared IR methods facing both the realistic and the real-world cases of study. From the latter results, both Evo-G&PR and SS are the methods that achieved the best performance according to the overall robustness of the methods tackling the point matching-based IR problem. This behavior is similar to that shown by both methods in terms of effectiveness (see Section 4.4).

Figure 10 represents the obtained results in a graphical way. For the sake of visual interpretation, different gray-scale colors are used to represent the scene and model images. The first column in Figure 10 corresponds to the initial configurations of the four different IR problem instances of MRIs. The next columns show the best IR results obtained by the compared methods: pure GRASP, Stc-G&PR, Dyn-G&PR, Evo-G&PR, and SS, respectively. Notice that the initial configurations considered correspond to important misalignment of the images. Hence, the IR problem instances tackled are really complex. Even dealing with such complex scenarios, both Evo-G&PR and SS methods achieve outstanding best solutions. That is visually shown by the almost perfect overlapping of the colors of the objects in the fifth and sixth columns of Figure 10. The visual results corresponding to the IR of CT images, i.e. I_6 vs. $T_1(I_5)$ (see Figure 11) show the high complexity of this real-world case of study, mainly originated by the nature of the anatomical structure of the human wrist. Again, it can be observed how the two said methods provide the best results.

Table 9: Statistical results computed from ten runs performed on each of the five IR problems considered. The minimum (m), maximum (M), mean (μ), and standard deviation (σ) values of MSE. The best results according to mean and standard deviation values are highlighted. The last row refers to the averaged performance considering the five IR problems at once

		Stc-G&PR	Dyn-G&PR	Evo-G&PR	GRASP	SS	
I_1 vs $T_1(I_2)$	<i>min</i>	46.59	40.82	41.79	44.09	39.70	
	<i>max</i>	59.14	49.38	47.26	58.27	45.53	
	μ	50.48	44.22	44.43	50.39	42.85	
	σ	4.23	2.42	1.86	4.84	1.88	
I_1 vs $T_2(I_3)$	<i>min</i>	42.37	39.93	39.17	44.16	40.77	
	<i>max</i>	64.85	49.58	45.05	91.74	49.71	
	μ	50.20	43.34	43.22	60.44	44.62	
	σ	6.45	2.77	1.76	13.59	2.23	
I_1 vs $T_3(I_4)$	<i>min</i>	81.37	58.66	57.41	83.25	57.37	
	<i>max</i>	100.57	64.51	62.73	141.04	64.90	
	μ	88.94	61.04	60.88	108.60	61.18	
	σ	6.15	1.76	1.57	18.62	1.88	
I_2 vs $T_4(I_4)$	<i>min</i>	120.22	85.32	81.00	136.10	78.70	
	<i>max</i>	168.34	105.52	91.89	228.06	95.02	
	μ	143.76	94.14	88.51	156.38	87.80	
	σ	14.74	6.12	3.59	26.49	5.19	
I_6 vs $T_1(I_5)$	<i>min</i>	1.87	1.74	1.68	2.26	1.63	
	<i>max</i>	3.47	1.89	1.95	3.57	3.99	
	μ	2.70	1.81	1.80	2.88	2.19	
	σ	0.52	0.04	0.10	0.44	0.83	
		μ	67.22	48.91	47.77	75.74	47.73

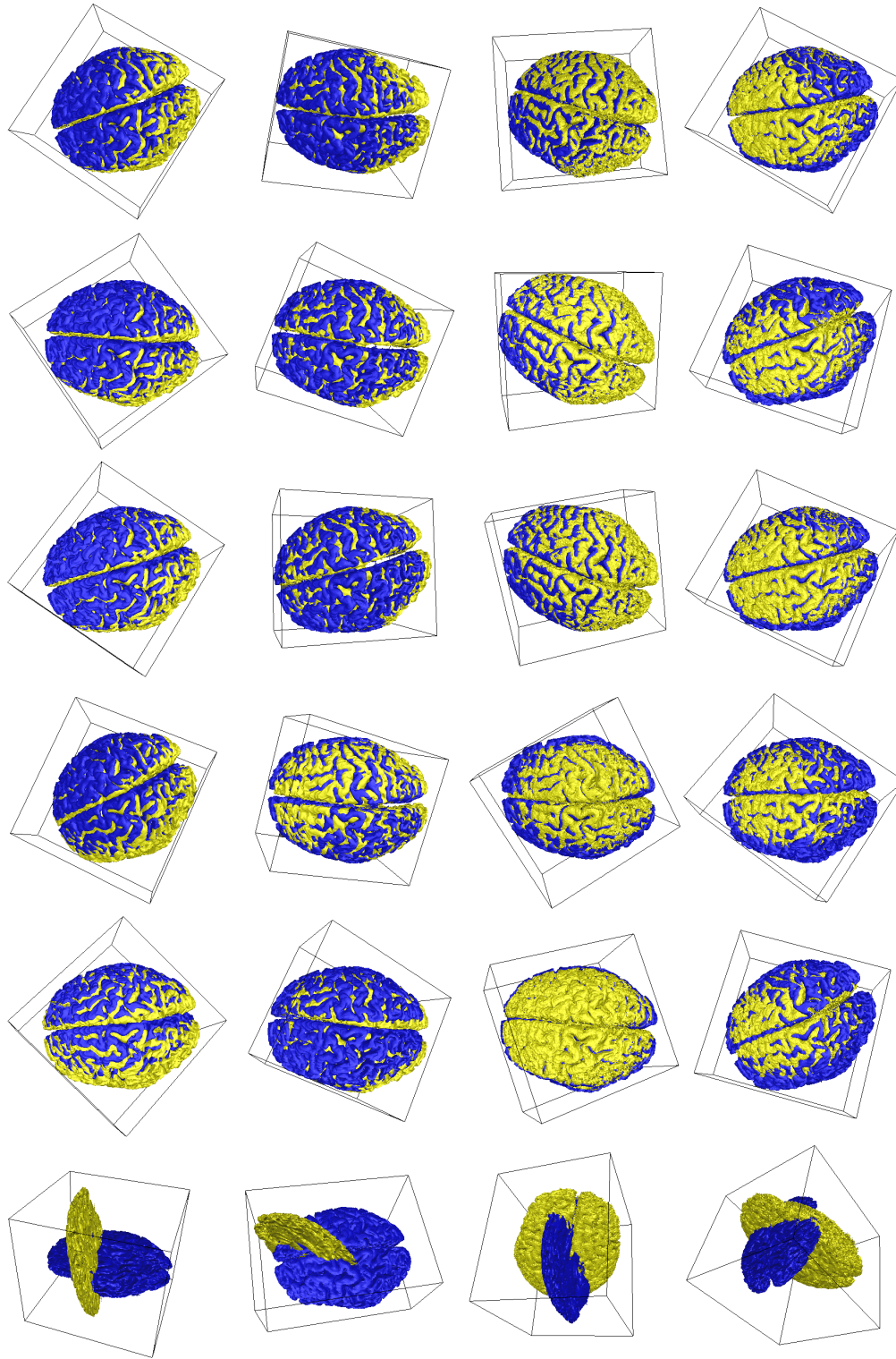


Figure 10: The first column graphically represent the four IR problem instances using MRIs (I_1 vs $T_1(I_2)$, I_1 vs $T_2(I_3)$, I_1 vs $T_3(I_4)$, and I_2 vs $T_4(I_4)$). From left to right, the next columns show the best IR results achieved by GRASP, Stc-G&PR, Dyn-G&PR, Evo-G&PR, and SS IR methods facing each IR problem, respectively

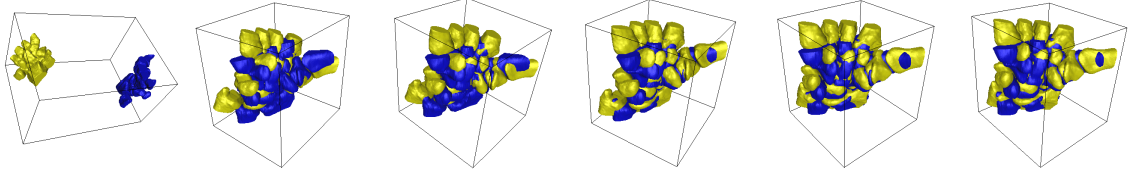


Figure 11: The first column graphically represent the IR problem instance using CT images (I_6 vs $T_1(I_5)$). From left to right, the next columns show the best IR results achieved by GRASP, Stc-G&PR, Dyn-G&PR, Evo-G&PR, and SS IR methods, respectively

5. Conclusions and future works

We presented a contribution facing a challenging real-world computer vision problem by means of recent hybridizations of GRASP and PR algorithms. Specifically, in this work we proposed several designs of advanced hybridizations to tackle the point matching-based IR problem based on a static, a dynamic, and an evolutionary approach.

Next, we studied the performance of these new IR methods in both realistic and real-world medical applications, using different image modalities as MRIs and CT images of human brains and human wrists, respectively. We proved how the synergy between the single and multiple trajectory approaches and the evolutionary scheme of PR provided effective and robust results which were competitive with the state-of-the-art point matching-base IR methods based on SS algorithm. A good trade-off between search space diversification and intensification have originated the high performance achieved by the new hybrid designs.

As future works, we consider the use of new hybrid designs based on GRASP and PR and similar approaches (Lozano and García-Martínez, 2010) for tackling the point matching-based IR problem in order to obtain more accurate and robust methods.

Acknowledgments

We want to acknowledge Professor J. J. Crisco for providing us the CT images of human wrists. This work was partially supported by the Spain’s Ministerio de Ciencia e Innovación (Ref. TIN2009-07727 and TIN2009-07516) and by the Andalusia’s Dpto. de Innovación, Ciencia y Empresa (Ref. TIC1619), both including EDRF fundings.

References

- Andrade, D. V., M G C. Resende. 2007. Grasp with evolutionary path-relinking. *7th Metaheuristics International Conference (MIC 2007)*.
- Arun, K. S., T. S. Huang, S. D. Blostein. 1987. Least-squares fitting of two 3-D points sets. *IEEE T. Pattern Anal.* **9** 698–700.
- Besl, P. J., N. D. McKay. 1992. A method for registration of 3D shapes. *IEEE T. Pattern Anal.* **14** 239–256.
- Brown, L. G. 1992. A survey of image registration techniques. *ACM Comput. Surv.* **24** 325–376.
- Cordón, O., S. Damas. 2006. Image Registration with Iterated Local Search. *J. Heuristics* **12** 73–94.
- Cordón, O., S. Damas, J. Santamaría. 2006a. A Fast and Accurate Approach for 3D Image Registration using the Scatter Search Evolutionary Algorithm. *Pattern Recogn. Lett.* **27** 1191–1200.
- Cordón, O., S. Damas, J. Santamaría. 2006b. Feature-based image registration by means of the CHC evolutionary algorithm. *Image Vision Comput.* **22** 525–533.
- Cordón, O., S. Damas, J. Santamaría. 2007. A practical review on the applicability of different EAs to 3D feature-based registration. S. Cagnoni, E. Lutton, G. Olague, eds., *Genetic and Evolutionary Computation in Image Processing and Computer Vision*. EURASIP Book Series on SP&C, 247–269.
- Cordón, O., S. Damas, J. Santamaría, R. Martí. 2008. Scatter Search for the 3D Point Matching Problem in Image Registration. *INFORMS J. Comput.* **20** 55–68.
- Dasgupta, S., A. Banerjee. 2005. Pattern tracking and 3-D motion reconstruction of a rigid body from a 2-D image sequence. *IEEE T. Syst. Man Cy. C* **35** 116–125.
- De Falco, I., A. Della Cioppa, D. Maisto, E. Tarantino. 2008. Differential Evolution as a viable tool for satellite image registration. *Appl. Soft Comput.* **8** 1453–1462.

- Faria, H., S. Binato, M. G. C. Resende, D. J. Falcao. 2005. Transmission network design by a greedy randomized adaptive path relinking approach. *IEEE Trans. Power Syst.* **20** 43–49.
- Feldmar, J., N. Ayache. 1996. Rigid, affine and locally affine registration of free-form surfaces. *Int. J. Comput. Vision* **18** 99–119.
- Feo, T. A., M. G. C. Resende. 1989. A probabilistic heuristic for a computationally difficult set covering problem. *Oper. Res. Lett.* **8** 67–71.
- Feo, T. A., M. G. C. Resende. 1995. Greedy randomized adaptive search procedures. *J. Global Optim.* **6** 109–133.
- Glover, F. 1996. Tabu search and adaptive memory programming – advances, applications and challenges. *Interfaces in Computer Science and Operations Research*. Kluwer, 1–75.
- Glover, F., G. A. Kochenberger, eds. 2003. *Handbook of Metaheuristics*. Kluwer Academic Publishers.
- Glover, F., M. Laguna. 1997. *Tabu Search*. Kluwer Academic Publishers.
- Glover, Fred. 1986. Future paths for integer programming and links to artificial intelligence. *Comput. Oper. Res.* **13** 533–549.
- González, R. C., R. E. Woods. 2002. *Digital Image Processing*. Prentice-Hall.
- Goshtasby, A. 2005. *2D and 3D Image Registration*. Wiley Interscience.
- He, R., P. A. Narayana. 2002. Global optimization of mutual information: application to three-dimensional retrospective registration of magnetic resonance images. *Comput. Med. Imag. Grap.* **26** 277–292.
- Horn, B. K. P. 1987. Closed-form solution of absolute orientation using unit quaternions. *J. Opt. Soc. Am.* **4** 629–642.
- Kim, J., S. Byun, B. Ahn. 2001. Fast full search motion estimation algorithm using various matching scans in video coding. *IEEE T. Syst. Man Cy. C* **31** 540–548.
- Kwan, R. K. S., A. C. Evans, G. B. Pike. 1999. MRI simulation-based evaluation of image-processing and classification methods. *IEEE T. Med. Imaging* **18** 1085–1097.

- Laguna, M., R. Martí. 1999. GRASP and Path Relinking for 2-layer Straight Line Crossing Minimization. *INFORMS J. Comput.* **11** 44–52.
- Liu, Y. 2004. Improving ICP with easy implementation for free form surface matching. *Pattern Recogn.* **37** 211–226.
- Lozano, M., C. García-Martínez. 2010. Hybrid metaheuristics with evolutionary algorithms specializing in intensification and diversification: Overview and progress report. *Comput. Oper. Res.* **37** 481–497.
- Luck, J. P., C. Q. Little, W. Hoff. 2000. Registration of Range Data Using a Hybrid Simulated Annealing and Iterative Closest Point Algorithm. *IEEE International Conference on Robotics and Automation (ICRA '00)*. 3739–3744.
- Marai, G. E., D. H. Laidlaw, J. J. Crisco. 2006. Super-Resolution Registration Using Tissue-Classified Distance Fields. *IEEE T. Med. Imaging* **25** 177–187.
- Monga, O., S. Benayoun, O. Faugeras. 1992. From partial derivatives of 3-D density images to ridges lines. *Computer Vision and Pattern Recognition*. IEEE, Champaign, Illinois, EEUU, 354–389.
- Prais, M., C. Ribeiro. 2000. Reactive GRASP: An Application to a Matrix Decomposition Problem in TDMA Traffic Assignment. *INFORMS J. Comput.* **12** 164–176.
- Resende, M. C., R. Martí, M. Gallego, A. Duarte. 2010. Grasp and path relinking for the max-min diversity problem. *Comput. Oper. Res.* **37** 498–508.
- Resende, M. C., C. C. Ribeiro. 2003. Greedy randomized adaptive search procedures. F. Glover, G. Kochenberger, eds., *Handbook of Metaheuristics*. Kluwer Academic Publishers, 219–249.
- Resende, M. C., R. F. Werneck. 2004. A hybrid heuristic for the p-median problem. *J. Heuristics* **10** 59–88.
- Robertson, C., R. B. Fisher. 2002. Parallel Evolutionary Registration of Range Data. *Comput. Vis. Image Underst.* **87** 39–50.

- Santamaría, J., O. Cordón, S. Damas, J.M. García-Torres, A. Quirin. 2009. Performance evaluation of memetic approaches in 3D reconstruction of forensic objects. *Soft Comput.* **13** 883–904.
- Santamaría, J., O. Cordón, S. Damas, R. Martí, R.J. Palma. 2010. GRASP & Evolutionary Path Relinking for Medical Image Registration based on Point Matching. *IEEE Congress on Evolutionary Computation 2010 (CEC 2010)*. Barcelona, Spain, In press.
- Silva, L., O. R. P. Bellon, K. L. Boyer. 2005. Precision range image registration using a robust surface interpenetration measure and enhanced genetic algorithms. *IEEE T. Pattern Anal.* **27** 762–776.
- Wachowiak, M. P., R. Smolikova, Y. Zheng, J. M. Zurada, A. S. El-Maghraby. 2004. An approach to multimodal biomedical image registration utilizing particle swarm optimization. *IEEE T. Evolut. Comput.* **8** 289–301.
- Wang, F. 2005. An efficient coordinate frame calibration method for 3-D measurement by multiple camera systems. *IEEE T. Syst. Man Cy. C* **35** 453–464.
- Yamany, S. M., M. N. Ahmed, A. A. Farag. 1999. A new genetic-based technique for matching 3D curves and surfaces. *Pattern Recogn.* **32** 1817–1820.
- Zitová, B., J. Flusser. 2003. Image registration methods: a survey. *Image Vision Comput.* **21** 977–1000.